

A Differential Theory of Radiative Transfer

ANONYMOUS AUTHOR(S)

SUBMISSION ID: XXX



Fig. 1. We need a nice teaser!

TBD.

Table 1. List of symbols commonly used in this paper.

1 INTRODUCTION

TBD

2 RELATED WORK

Differentiable rendering. [Li et al. 2018]

3 PRELIMINARIES

We now briefly revisit the radiative transfer framework (§3.1) and outline how the radiances given by this framework can be differentiated with respect to scene geometry (§3.2, §3.3).

3.1 Radiative Transfer

Radiative transfer [Chandrasekhar 2013] has been used to model light transport in participating media in many fields including biomedical imaging, remote sensing, and computer graphics.

At the core of the radiative transfer framework is the *radiative transfer equation* (RTE) that takes the form of a linear transport equation. Specifically, for a medium that (i) has *extinction coefficient* σ_t , *scattering coefficient* σ_s , and *single-scattering phase function* f_p ; and (ii) is contained in $\Omega \subseteq \mathbb{R}^3$ with boundary $\partial\Omega$, the RTE states that the *radiance field* L interior of the medium satisfies

$$L = \mathcal{K}_T \mathcal{K}_C L + Q. \quad (1)$$

For any $g : (\Omega \setminus \partial\Omega) \times \mathbb{S}^2 \rightarrow \mathbb{R}_+$, \mathcal{K}_T is the *transport operator* given by

$$(\mathcal{K}_T g)(\mathbf{x}, \omega) = \int_0^D T(\mathbf{x}', \mathbf{x}) \sigma_s(\mathbf{x}') g(\mathbf{x}', \omega) d\tau, \quad (2)$$

where $\mathbf{x}' := \mathbf{x} - \tau\omega$,

$$D := \inf\{\tau \in \mathbb{R}_+ : \mathbf{x} - \tau\omega \in \partial\Omega\}, \quad (3)$$

and $T(\mathbf{x}', \mathbf{x})$ denotes the *transmittance* between \mathbf{x}' and \mathbf{x} that equals

$$T(\mathbf{x}', \mathbf{x}) = \exp\left(-\int_0^\tau \sigma_t(\mathbf{x} - \tau'\omega) d\tau'\right). \quad (4)$$

Symbol	Meaning	Def.
L, L_s	interior and interfacial radiances	(1, 7)
L^{ins}	in-scattered radiance (interior)	(5)
L_s^e	emitted radiance (interfacial)	(7)
L_s^r	reflected/refracted radiance (interfacial)	(??)
$L^{(1)}, L^{(0)}$	indirect and direct radiances (interior)	(??, 10)
$\Omega(t)$	time-varying domain	(12)
$\partial\Omega(t)$	time-varying domain boundary	(12)
\dot{f}	time-derivative of f (i.e., $\frac{\partial}{\partial t}f$)	(12)
$\mathbf{x}', \dot{\mathbf{x}}'$	$\mathbf{x} - \tau\omega, \dot{\mathbf{x}} - \tau\dot{\omega}$	(1, ??)
$\mathbf{x}_0, \dot{\mathbf{x}}_0$	$\mathbf{x} - D\omega, \dot{\mathbf{x}} - \dot{D}\omega$	(1, ??)
$\langle \mathbf{u}, \mathbf{v} \rangle$	dot (inner) product between vectors \mathbf{u} and \mathbf{v}	(12)
$\mathbf{x} \rightarrow \mathbf{y}$	unit vector pointing from \mathbf{x} to \mathbf{y} , i.e., $\frac{\mathbf{y}-\mathbf{x}}{\ \mathbf{y}-\mathbf{x}\ }$	(29)

Further, \mathcal{K}_C in Eq. (1) is the *collision operator* which, when applied to the interior radiance field L , gives the *in-scattered radiance* L^{ins} as follows:¹

$$L^{\text{ins}}(\mathbf{x}, \omega) = (\mathcal{K}_C L)(\mathbf{x}, \omega) = \int_{\mathbb{S}^2} f_p(\mathbf{x}, -\omega', \omega) L(\mathbf{x}, \omega') d\omega'. \quad (5)$$

Lastly, the *source term* Q of the RTE (1) is given by²

$$Q(\mathbf{x}, \omega) = T(\mathbf{x}_0, \mathbf{x}) L_s(\mathbf{x}_0, \omega), \quad (6)$$

where $\mathbf{x}_0 := \mathbf{x} - D\omega$, and L_s indicates the *interfacial radiance* that serves as the boundary condition of the RTE (1) and satisfies the *rendering equation* (RE) for all $\mathbf{x} \in \partial\Omega$ and $\omega \in \mathbb{S}^2$:

$$L_s(\mathbf{x}, \omega) = \underbrace{\int_{\mathbb{S}^2} f_s(\mathbf{x}, -\omega', \omega) L(\mathbf{x}, \omega') d\omega'}_{=: L_s^r(\mathbf{x}, \omega)} + L_s^e(\mathbf{x}, \omega), \quad (7)$$

¹In this paper, we follow the convention that all directions point away from \mathbf{x} , yielding the negative sign before ω' in Eq. (5).

²When Ω is unbounded, D can be infinite for certain \mathbf{x} and ω , leading to $Q(\mathbf{x}, \omega) = 0$.

where f_s is the *cosine-weighted BSDF*, L_s^e denotes the *emitted radiance*, and L_s^r indicates the *reflected/refracted radiance*. Please refer to Table 1 for a summary of all commonly used symbols.

Combining the RTE and the RE. According to Eqs. (6, 7), the source term Q of the RTE (1) can be rewritten as

$$Q = \mathcal{K}_S L + L^{(0)}, \quad (8)$$

where \mathcal{K}_S is termed as the *interfacial scattering operator* satisfying

$$\begin{aligned} (\mathcal{K}_S L)(\mathbf{x}, \boldsymbol{\omega}) &= T(\mathbf{x}_0, \mathbf{x}) L_s^r(\mathbf{x}_0, \boldsymbol{\omega}) \\ &= T(\mathbf{x}_0, \mathbf{x}) \int_{\mathbb{S}^2} f_s(\mathbf{x}_0, -\boldsymbol{\omega}', \boldsymbol{\omega}) L(\mathbf{x}_0, \boldsymbol{\omega}') d\boldsymbol{\omega}', \end{aligned} \quad (9)$$

and

$$L^{(0)}(\mathbf{x}, \boldsymbol{\omega}) := T(\mathbf{x}_0, \mathbf{x}) L_s^e(\mathbf{x}_0, \boldsymbol{\omega}). \quad (10)$$

According to Eqs. (8–10), the RTE (1) can be rewritten as an equation that only depends on the interior radiance L :

$$L = (\mathcal{K}_T \mathcal{K}_C + \mathcal{K}_S) L + L^{(0)}. \quad (11)$$

3.2 Shape Derivatives

This paper focuses on the problem of differentiating L with respect to scene geometries (depicted with Ω and $\partial\Omega$) or camera poses. To this end, we model Ω and $\partial\Omega$ as *time-varying* quantities, a common practice in shape optimization [Zhao et al. 2018]. This causes the radiance L , as the solutions to the RTE (11), to also be time-varying.³ Further, the differential changes of L with respect to Ω and $\partial\Omega$ are fully captured by the corresponding *time derivative* \dot{L} .

Specifically, we use $\Omega(t)$ and $\partial\Omega(t)$ to denote the time-varying geometries. For each point $\mathbf{x}(t) \in \partial\Omega(t)$, its velocity at time t is given by $\mathbf{v}(\mathbf{x}, t) = \dot{\mathbf{x}}(t)$ where $\dot{\mathbf{x}}$ denotes the time derivative of \mathbf{x} . In this paper, we assume Ω , $\partial\Omega$, and $\dot{\mathbf{x}}$ to be given and focus on estimating the resulting derivative \dot{L} .

3.3 Differentiating Integrals over Manifolds

Deriving the time derivatives of radiances requires differentiating the integrals from the RTE (1) and the RE (7). To this end, we utilize the Reynolds transport theorem [Leal 2007] originated in fluid mechanics. Compared to the work by Li et al. [2018], our derivations enjoy (i) a cleaner top-down structure; and (ii) the generality to support subsurface scattering.

THEOREM 1 (REYNOLDS TRANSPORT THEOREM). *Let $\Omega(t)$ be some evolving n -dimensional manifold with boundary $\partial\Omega(t)$ and boundary velocity $\mathbf{v}(t)$ at time t . Then, for some function $f(\mathbf{x}, t)$ continuous in \mathbf{x} and t , it holds that*

$$\frac{\partial}{\partial t} \left(\int_{\Omega(t)} f d\Omega(t) \right) = \int_{\Omega(t)} \dot{f} d\Omega(t) + \int_{\partial\Omega(t)} \langle \mathbf{n}, \mathbf{v} \rangle f d(\partial\Omega(t)), \quad (12)$$

where $\dot{f} := \frac{\partial}{\partial t} f$; $d\Omega$ and $d(\partial\Omega)$ respectively denote the measures induced by Ω and $\partial\Omega$; \mathbf{n} indicates the time-varying normal direction for each boundary point (that points toward the exterior of Ω); and $\langle \cdot, \cdot \rangle$ denotes the dot (inner) product between a pair of vectors.

³Despite making Ω and $\partial\Omega$ time-varying, we keep using steady-state RTE that assumes L to reach equilibrium instantaneously.

In a special case, for classical Riemann integrals where Ω is an interval $(a, b) \subset \mathbb{R}$, it holds that $\partial\Omega = \{a, b\}$, and the boundary integral in Eq. (12) reduces to the sum of the integrand evaluated at a and b . Additionally, it is easy to verify that $\langle \mathbf{n}, \mathbf{v} \rangle$ equals \dot{b} at $x = b$ and $-\dot{a}$ at $x = a$, yielding

$$\begin{aligned} \frac{\partial}{\partial t} \int_{a(t)}^{b(t)} f(x, t) dx &= \int_{a(t)}^{b(t)} \dot{f}(x, t) dx \\ &\quad + \dot{b}(t) f(b(t), t) - \dot{a}(t) f(a(t), t), \end{aligned} \quad (13)$$

which is precisely the well-known Leibniz's rule for differentiation [Flanders 1973].

For integrands with internal discontinuities, one can partition the integral domain $\Omega(t)$ so that the function remains piecewise continuous, leading to the following corollary.

COROLLARY 2. *Let f be a scalar-valued function defined on some evolving n -dimensional manifold $\Omega(t)$ with “interface” $\Gamma(t)$, an $(n-1)$ -dimensional submanifold given by the union of the external boundary $\partial\Omega(t)$ and the internal one containing the discontinuous locations of f at time t . Then, given interfacial velocity $\mathbf{v}(t)$, it holds that*

$$\frac{\partial}{\partial t} \left(\int_{\Omega(t)} f d\Omega(t) \right) = \int_{\Omega(t)} \dot{f} d\Omega(t) + \int_{\Gamma(t)} |\langle \mathbf{n}, \mathbf{v} \rangle| \Delta f d\Gamma(t), \quad (14)$$

where^a

$$\Delta f(\mathbf{x}) := \lim_{\epsilon \rightarrow 0^-} f(\mathbf{x} + \epsilon \mathbf{v}(\mathbf{x})) - \lim_{\epsilon \rightarrow 0^+} f(\mathbf{x} + \epsilon \mathbf{v}(\mathbf{x})), \quad (15)$$

for all $\mathbf{x} \in \Gamma(t)$. As a special case, when \mathbf{x} approaches $\Gamma(t)$ from the external of $\Omega(t)$, the corresponding one-sided limit in Eq. (15) is set to zero.

^aIn Eq. (15), the time-dependencies of f , \mathbf{x} , and \mathbf{v} are omitted for notational convenience.

In the rest of this paper, we detail how Corollary 2 can be used to calculate time derivatives of radiances in §4 and introduce unbiased Monte Carlo estimators for these derivatives in §5.

4 DIFFERENTIABLE RADIATIVE TRANSFER

In this section, we derive \dot{L} , time derivatives of the interior radiance L , by differentiating Eq. (11) using Corollary 2.

To simplify the derivations, similar to the work by Li et al. [2018], we assume that: (i) the RTE and RE parameters σ_t , σ_s , f_p , f_s , and L_s^e are continuous and time-independent; and (ii) there is no delta light sources (e.g., point and directional) or ideal specular surfaces (e.g., perfect mirrors). We discuss how these assumptions can be relaxed in §6.

4.1 Overview

We now analyze the differentiation of interior radiance L at the operator level. Let $\mathcal{K} := \mathcal{K}_T \mathcal{K}_C + \mathcal{K}_S$, the RTE (11) can be rewritten as $L = \mathcal{K} L + L^{(0)}$, whose time derivative is

$$\dot{L} = \frac{\partial}{\partial t} (\mathcal{K} L + L^{(0)}) = \frac{\partial}{\partial t} (\mathcal{K} L) + \dot{L}^{(0)}. \quad (16)$$

Outline of Our Derivations

$$\dot{L} = \underbrace{\frac{\partial}{\partial t} \mathcal{K}_T \mathcal{K}_C L}_{\S 4.2} + \underbrace{\frac{\partial}{\partial t} \mathcal{K}_S L}_{\S 4.4} + \underbrace{\dot{L}^{(0)}}_{\S 4.5}.$$

Fig. 2. An **outline of our derivations** in §4. To derive \dot{L} , we differentiate the transport operator \mathcal{K}_T in §4.2, the collision operator \mathcal{K}_C in §4.3, the interfacial scattering operator \mathcal{K}_S in §4.4, and the source term $L^{(0)}$ in §4.5.

As the operator \mathcal{K} involves multiple integrals, according to Corollary 2, we know that the time derivative of $\mathcal{K}L$ takes the form

$$\frac{\partial}{\partial t}(\mathcal{K}L) = \dot{\mathcal{K}}L + \mathcal{K}\dot{L} + \mathcal{K}_B L = (\dot{\mathcal{K}} + \mathcal{K}_B)L + \mathcal{K}\dot{L}, \quad (17)$$

where $\mathcal{K}_B L$ arises from differentiating non-radiance terms as well as the boundary integrals in Eqs. (12, 14).

Let $\mathcal{K}_0 := \dot{\mathcal{K}} + \mathcal{K}_B$. Combining Eqs. (16, 17) yields a linear transport equation of \dot{L} :

$$\dot{L} = \mathcal{K}\dot{L} + \mathcal{K}_0 L + \dot{L}^{(0)}, \quad (18)$$

which we term as the *differential radiative transfer equation* (DRTE). The solution \dot{L} of the DRTE can be expressed as a Neumann series of the form

$$\dot{L} = \sum_{n=0}^{\infty} \mathcal{K}^n (\mathcal{K}_0 L + \dot{L}^{(0)}). \quad (19)$$

Despite the conceptually simple derivation of the DRTE (18), the actual form of \dot{L} is complicated due to the complexity of the operators involved (i.e., \mathcal{K}_T , \mathcal{K}_C , and \mathcal{K}_S). In the rest of this section, we derive the differential forms of these operators individually. Figure 2 outlines the structure of our derivations.

In practice, what we generally need is to estimate \dot{L} at some specific time t . Thus, without loss of generality, we focus on the derivatives at $t = 0$ in the rest of this paper.

4.2 Differentiation of the Transport Operator

The first term of Figure 2, i.e., $\frac{\partial}{\partial t} \mathcal{K}_T \mathcal{K}_C L = \frac{\partial}{\partial t} \mathcal{K}_T L^{\text{ins}}$ involves differentiating the transport operator \mathcal{K}_T . Given potentially *time-varying*⁴ $\mathbf{x} \in \Omega \setminus \partial\Omega$ and $\boldsymbol{\omega} \in \mathbb{S}^2$, it holds that

$$\begin{aligned} \left(\frac{\partial}{\partial t} \mathcal{K}_T L^{\text{ins}} \right)(\mathbf{x}, \boldsymbol{\omega}) &= \int_0^D T(\mathbf{x}', \mathbf{x}) \sigma_s(\mathbf{x}') \dot{L}^{\text{ins}}(\mathbf{x}', \boldsymbol{\omega}) d\tau \\ &+ \int_0^D \frac{\partial}{\partial t} [T(\mathbf{x}', \mathbf{x}) \sigma_s(\mathbf{x}')] L^{\text{ins}}(\mathbf{x}', \boldsymbol{\omega}) d\tau \\ &+ \dot{D} T(\mathbf{x}_0, \mathbf{x}) \sigma_s(\mathbf{x}_0) L^{\text{ins}}(\mathbf{x}_0, \boldsymbol{\omega}), \end{aligned} \quad (20)$$

with $\mathbf{x}' := \mathbf{x} - \tau\boldsymbol{\omega}$, and $\mathbf{x}_0 = \mathbf{x} - D\boldsymbol{\omega}$. Notice that, the assumptions expressed at the beginning of this section ensures the integrand of $\mathcal{K}_T L^{\text{ins}}$ to be continuous in τ for $0 < \tau < D$, allowing us to differentiate $\mathcal{K}_T L^{\text{ins}}$ using Theorem 1. We discuss the generalized forms of Eq. (20) in §6.1.

⁴We allow both \mathbf{x} and $\boldsymbol{\omega}$ to be time-varying in our derivations for handling scenes with moving cameras. Please refer to §4.6 to more details.

To derive $\frac{\partial}{\partial t} T(\mathbf{x}', \mathbf{x}) \sigma_s(\mathbf{x}')$, we have

$$\dot{\sigma}_s(\mathbf{x}') = \langle \nabla \sigma_s(\mathbf{x}'), \dot{\mathbf{x}}' \rangle, \quad (21)$$

where $\dot{\mathbf{x}}' = \dot{\mathbf{x}} - \tau\dot{\boldsymbol{\omega}}$ and

$$\dot{T}(\mathbf{x}', \mathbf{x}) = \frac{\partial}{\partial t} \exp \left(- \int_0^\tau \sigma_t(\mathbf{x}'') d\tau' \right) = -T(\mathbf{x}', \mathbf{x}) \Sigma_t(\mathbf{x}, \boldsymbol{\omega}, \tau), \quad (22)$$

where $\mathbf{x}'' := \mathbf{x} - \tau'\boldsymbol{\omega}$, $\dot{\mathbf{x}}'' = \dot{\mathbf{x}} - \tau'\dot{\boldsymbol{\omega}}$, and

$$\Sigma_t(\mathbf{x}, \boldsymbol{\omega}, \tau) := \int_0^\tau \dot{\sigma}_t(\mathbf{x}'') d\tau' = \int_0^\tau \langle \nabla \sigma_t(\mathbf{x}''), \dot{\mathbf{x}}'' \rangle d\tau'. \quad (23)$$

Lastly, combining Eqs. (20–23) gives

$$\begin{aligned} \left(\frac{\partial}{\partial t} \mathcal{K}_T L^{\text{ins}} \right)(\mathbf{x}, \boldsymbol{\omega}) &= \int_0^D T(\mathbf{x}', \mathbf{x}) \sigma_s(\mathbf{x}') \dot{L}^{\text{ins}}(\mathbf{x}', \boldsymbol{\omega}) d\tau \\ &+ \int_0^D T(\mathbf{x}', \mathbf{x}) (\dot{\sigma}_s(\mathbf{x}') - \Sigma_t(\mathbf{x}, \boldsymbol{\omega}, \tau) \sigma_s(\mathbf{x}')) L^{\text{ins}}(\mathbf{x}', \boldsymbol{\omega}) d\tau \\ &+ \dot{D} T(\mathbf{x}_0, \mathbf{x}) \sigma_s(\mathbf{x}_0) L^{\text{ins}}(\mathbf{x}_0, \boldsymbol{\omega}), \end{aligned} \quad (24)$$

where \dot{D} , $L^{\text{ins}}(\mathbf{x}_0, \boldsymbol{\omega})$, and $\dot{L}^{\text{ins}}(\mathbf{x}', \boldsymbol{\omega})$ are derived in §4.2.1, §4.2.2, and §4.3, respectively.

At a high level, the last two terms on the RHS of Eq. (24) correspond to the \mathcal{K}_0 operator in the DRTE (18) while the first one to both \mathcal{K} and \mathcal{K}_0 .

4.2.1 Derivation of \dot{D} . Differentiating $\mathcal{K}_T L^{\text{ins}}$ requires calculating \dot{D} , the change rate of the line integral's upper-bound.

Given \mathbf{x} and $\boldsymbol{\omega}$, assume that the boundary $\partial\Omega(t)$ has an implicit representation $F(\mathbf{y}, t) = 0$ locally around the intersection with the ray $(\mathbf{x}, -\boldsymbol{\omega})$.⁵ Then, substituting \mathbf{y} with the ray equation yields

$$F(\mathbf{x} - D\boldsymbol{\omega}, t) = 0. \quad (25)$$

Assuming the (minimal positive) solution to this equation to be $D(t)$, then $\dot{D} = \frac{\partial}{\partial t} D|_{t=0}$. For instance, for a plane with normal \mathbf{n} that translates uniformly with velocity \mathbf{v} , $\dot{D} = \langle \mathbf{n}, \dot{\mathbf{x}} - \mathbf{v} \rangle / \langle \mathbf{n}, \boldsymbol{\omega} \rangle$.

Please refer to Appendix B for detailed derivations of \dot{D} under a few configurations. In general, when $D(t)$ has an analytical form, \dot{D} can be obtained via *symbolic/automated differentiation*.

4.2.2 Boundary in-scattered radiance. The time derivative of $\mathcal{K}_T L^{\text{ins}}$ expressed in Eqs. (20, 24) also involves the in-scattered radiance L^{ins} evaluated at some boundary location \mathbf{x}_0 . This term arises from the boundary term of Reynolds' theorem (12).

To properly obtain $L^{\text{ins}}(\mathbf{x}_0, \boldsymbol{\omega})$ that includes an integral of (phase-function-modulated) radiance over all directions, the calculation needs to be restricted to the same side of the boundary as \mathbf{x} . Precisely, let $\mathbb{H}_+ := \{\boldsymbol{\omega}' \in \mathbb{S}^2 : \langle \mathbf{n}(\mathbf{x}_0), \boldsymbol{\omega}' \rangle > 0\}$, and $\mathbb{H}_- := \{\boldsymbol{\omega}' \in \mathbb{S}^2 : \langle \mathbf{n}(\mathbf{x}_0), \boldsymbol{\omega}' \rangle < 0\}$, where $\mathbf{n}(\mathbf{x}_0)$ denotes the surface normal at \mathbf{x}_0 with $\langle \mathbf{n}(\mathbf{x}_0), \boldsymbol{\omega} \rangle < 0$. Then, as illustrated in Figure 3, we have

$$\begin{aligned} L^{\text{ins}}(\mathbf{x}_0, \boldsymbol{\omega}) &= \int_{\mathbb{H}_+} f_p(\mathbf{x}_0, -\boldsymbol{\omega}', \boldsymbol{\omega}) L(\mathbf{x}_0, \boldsymbol{\omega}') d\boldsymbol{\omega}' \\ &+ \int_{\mathbb{H}_-} f_p(\mathbf{x}_0, -\boldsymbol{\omega}', \boldsymbol{\omega}) L_s(\mathbf{x}_0, \boldsymbol{\omega}') d\boldsymbol{\omega}'. \end{aligned} \quad (26)$$

⁵The existence of F is guaranteed by the implicit function theorem.

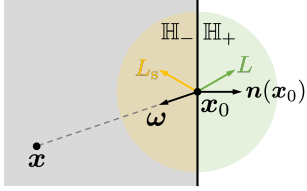


Fig. 3. Calculating the in-scattered radiance L^{ins} at location $\mathbf{x}_0 \in \partial\Omega$ with direction ω pointing toward the interior of the medium (illustrated in gray).

4.3 Differentiation of the Collision Operator

We now derive the time derivative of the in-scattered radiance $L^{\text{ins}} = \mathcal{K}_C L$ defined in Eq. (5). Since $L(\mathbf{x}, \omega)$ generally has jump discontinuities in ω (for fixed \mathbf{x}) due to visibility changes, we use Corollary 2 to derive \dot{L}^{ins} .

Let $\mathbb{S}(\mathbf{x}) \subset \mathbb{S}^2$ to be a set of *spherical curves* capturing all discontinuous locations of $f_p(\mathbf{x}, -\omega', \omega) L(\mathbf{x}, \omega')$ in ω' .⁶ Then, for $\mathbf{x} \in \Omega \setminus \partial\Omega$ and $\omega \in \mathbb{S}^2$ that are potentially time-varying, we have

$$\begin{aligned} \dot{L}^{\text{ins}}(\mathbf{x}, \omega) = & \int_{\mathbb{S}^2} f_p(\mathbf{x}, -\omega', \omega) \dot{L}(\mathbf{x}, \omega') d\omega' + \\ & \int_{\mathbb{S}^2} \dot{f}_p(\mathbf{x}, -\omega', \omega) L(\mathbf{x}, \omega') d\omega' + \\ & \int_{\mathbb{S}(\mathbf{x})} |\langle \mathbf{n}, \dot{\omega}' \rangle| f_p(\mathbf{x}, -\omega', \omega) \Delta L(\mathbf{x}, \omega') d\ell(\omega'), \end{aligned} \quad (27)$$

where $\mathbf{n}, \dot{\omega}'$ respectively denote the normal and velocity of $\mathbb{S}(\mathbf{x})$ at ω' and are derived below; ℓ indicates the curve-length measure; and

$$\begin{aligned} \Delta L(\mathbf{x}, \omega') = & \lim_{\epsilon \rightarrow 0^-} L(\mathbf{x} + \epsilon \dot{\mathbf{x}}, \omega' + \epsilon \dot{\omega}') \\ & - \lim_{\epsilon \rightarrow 0^+} L(\mathbf{x} + \epsilon \dot{\mathbf{x}}, \omega' + \epsilon \dot{\omega}'). \end{aligned} \quad (28)$$

In Eq. (27), $f_p(\mathbf{x}, -\omega', \omega)$ can be time-varying in general despite having time-independent formulation. Similar to \dot{D} , $\dot{f}_p(\mathbf{x}, -\omega', \omega)$ can generally be obtained using symbolic/automated differentiation.

Additionally, it is usually desired to have the last integral in Eq. (30) to be defined over a subset of $\partial\Omega$. To this end, let $\partial\Omega(\mathbf{x}) \subset \partial\Omega$ to denote all the *geometric edges* that can cause discontinuities when viewed from \mathbf{x} . Specifically, these include all *boundary* and *silhouette* edges (i.e., those shared by one front- and one back-facing faces). Then, it holds that

$$\begin{aligned} & \int_{\mathbb{S}(\mathbf{x})} |\langle \mathbf{n}, \dot{\omega}' \rangle| f_p(\mathbf{x}, -\omega', \omega) \Delta L(\mathbf{x}, \omega') d\ell(\omega') \\ = & \int_{\partial\Omega(\mathbf{x})} \left| \left\langle \mathbf{n}, \frac{\partial}{\partial t}(\mathbf{y} \rightarrow \mathbf{x}) \right\rangle \right| f_p(\mathbf{x}, \mathbf{x} \rightarrow \mathbf{y}, \omega) \\ & \Delta L(\mathbf{x}, \mathbf{y} \rightarrow \mathbf{x}) V(\mathbf{x}, \mathbf{y}) \frac{\sin \theta}{\|\mathbf{y} - \mathbf{x}\|} d\ell(\mathbf{y}), \end{aligned} \quad (29)$$

where $\mathbf{y} \rightarrow \mathbf{x}$ indicates the normalized direction from \mathbf{y} to \mathbf{x} , $V(\mathbf{x}, \mathbf{y})$ denotes the mutual visibility between \mathbf{x} and \mathbf{y} , and θ is the angle between the tangent direction at \mathbf{y} and $\mathbf{y} \rightarrow \mathbf{x}$. Previously, this change-of-measure term (i.e., $\sin \theta / \|\mathbf{y} - \mathbf{x}\|$) was also used by Li et al. [2018].

⁶Since we assume the phase function f_p to be continuous, $\mathbb{S}(\mathbf{x})$ is solely determined by the discontinuity of L .

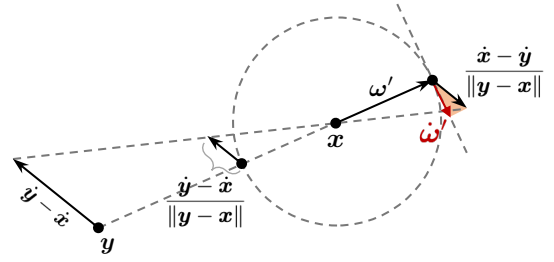


Fig. 4. Calculate projected velocity $\dot{\omega}'$. Given the velocity of \mathbf{y} relative to \mathbf{x} , i.e., $\dot{\mathbf{y}} - \dot{\mathbf{x}}$, one needs to (i) project it to the surface of a unit sphere centered at \mathbf{x} , yielding $(\dot{\mathbf{y}} - \dot{\mathbf{x}}) / \|\mathbf{y} - \mathbf{x}\|$; (ii) invert the projected velocity to align it with ω' , yielding $(\dot{\mathbf{x}} - \dot{\mathbf{y}}) / \|\mathbf{y} - \mathbf{x}\|$; and (iii) take the component (illustrated in red) of the inverted velocity that is within the tangent plane at ω' , yielding $\dot{\omega}'$ expressed in Eq. (32).

Combining Eqs. (27, 29) yields

$$\begin{aligned} \dot{L}^{\text{ins}}(\mathbf{x}, \omega) = & \int_{\mathbb{S}^2} f_p(\mathbf{x}, -\omega', \omega) \dot{L}(\mathbf{x}, \omega') d\omega' + \\ & \int_{\mathbb{S}^2} \dot{f}_p(\mathbf{x}, -\omega', \omega) L(\mathbf{x}, \omega') d\omega' + \\ & \int_{\partial\Omega(\mathbf{x})} \left| \left\langle \mathbf{n}, \frac{\partial}{\partial t}(\mathbf{y} \rightarrow \mathbf{x}) \right\rangle \right| f_p(\mathbf{x}, \mathbf{x} \rightarrow \mathbf{y}, \omega) \\ & \Delta L(\mathbf{x}, \mathbf{y} \rightarrow \mathbf{x}) V(\mathbf{x}, \mathbf{y}) \frac{\sin \theta}{\|\mathbf{y} - \mathbf{x}\|} d\ell(\mathbf{y}), \end{aligned} \quad (30)$$

where $\mathbf{n}, \frac{\partial}{\partial t}(\mathbf{y} \rightarrow \mathbf{x}) = \dot{\omega}'$, and ΔL are further derived below.

At a high level, the first integral in Eq. (30) contributes to the \mathcal{K} operator in the DRTE (18) while the remaining two join \mathcal{K}_0 . Another important observation is that, even when ω is time-varying, ω' for $\dot{L}(\mathbf{x}, \omega')$ and $L(\mathbf{x}, \omega')$ in Eq. (30) is *time-independent* as it arises from integrals that are constantly over \mathbb{S}^2 .

Normal and velocity. We now derive the normal \mathbf{n} and velocity $\dot{\omega}'$ in Eqs. (30, 29). The normal \mathbf{n} , which always lies in the tangent plane at ω' , relies on the geometry of $\partial\Omega(\mathbf{x})$. In case of polygonal meshes, $\partial\Omega(\mathbf{x})$ is comprised of individual face edges. For each edge segment with endpoints \mathbf{p} and \mathbf{q} , its projection on a unit sphere centered at \mathbf{x} is an arc with normal

$$\mathbf{n} = \frac{(\mathbf{p} - \mathbf{x}) \times (\mathbf{q} - \mathbf{x})}{\|(\mathbf{p} - \mathbf{x}) \times (\mathbf{q} - \mathbf{x})\|}. \quad (31)$$

For any point \mathbf{y} on the segment (\mathbf{p}, \mathbf{q}) with velocity $\dot{\mathbf{y}}$, let $\omega' = \mathbf{y} \rightarrow \mathbf{x}$. Then the velocity of ω' caused by that of \mathbf{x} and \mathbf{y} equals

$$\dot{\omega}' = \frac{\partial}{\partial t}(\mathbf{y} \rightarrow \mathbf{x}) = \dot{\mathbf{v}}(\mathbf{y}) - \omega' \langle \dot{\mathbf{v}}(\mathbf{y}), \omega' \rangle, \quad (32)$$

where $\dot{\mathbf{v}}(\mathbf{y}) := (\dot{\mathbf{x}} - \dot{\mathbf{y}}) / \|\mathbf{y} - \mathbf{x}\|$, as illustrated in Figure 4.

Calculating ΔL . The discontinuities of $L(\mathbf{x}, \omega')$ in ω' , with the absence of delta light sources and ideal specular surfaces, generally means the corresponding integral bounds d to be also discontinuous.

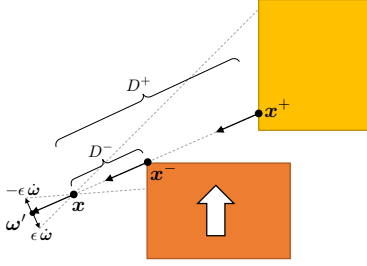


Fig. 5. Calculating ΔL . In this 2D example, the orange rectangle is translating upward with a constant velocity, and its top-left corner creates a geometric discontinuity when viewed from \mathbf{x} (that is stationary). Let ω' to denote the direction corresponding to this discontinuity (i.e., the ray $(\mathbf{x}, -\omega')$ intersects the orange rectangle at its top-left corner). Then, ω' rotates counterclockwise with some velocity $\dot{\omega}'$. Based on these observations, D^- , D^+ , \mathbf{x}^- , and \mathbf{x}^+ defined in Eqs. (33, 34) are illustrated.

For each $\omega' \in \mathbb{S}(\mathbf{x})$, let

$$\begin{aligned} D^- &:= \lim_{\epsilon \rightarrow 0^-} D(\mathbf{x} + \epsilon \dot{\mathbf{x}}, \omega' + \epsilon \dot{\omega}'), \\ D^+ &:= \lim_{\epsilon \rightarrow 0^+} D(\mathbf{x} + \epsilon \dot{\mathbf{x}}, \omega' + \epsilon \dot{\omega}'), \end{aligned} \quad (33)$$

and

$$\mathbf{x}^- := \mathbf{x} - D^- \omega', \quad \mathbf{x}^+ := \mathbf{x} - D^+ \omega'. \quad (34)$$

Then, it holds that

$$\begin{aligned} \Delta L(\mathbf{x}, \omega') &= \int_{D^+}^{D^-} T(\mathbf{x}', \mathbf{x}) \sigma_s(\mathbf{x}') L^{\text{ins}}(\mathbf{x}', \omega') d\tau \\ &\quad + T(\mathbf{x}^-, \mathbf{x}) L_s(\mathbf{x}^-, \omega') - T(\mathbf{x}^+, \mathbf{x}) L_s(\mathbf{x}^+, \omega'). \end{aligned} \quad (35)$$

Notice that it is possible for $D^+ > D^-$. In this case, the integral on the RHS of Eq. (35) takes a negative value. Figure 5 illustrates a 2D example for calculating ΔL .

4.4 Differentiation of the Interfacial Scattering Operator

We now derive the third term in Figure 2, the time derivative of $\mathcal{K}_S L$ given by Eq. (9).

Let $\mathbf{x}_0 := \mathbf{x} - D\omega$, then $\dot{\mathbf{x}}_0 = \frac{\partial}{\partial t}(\mathbf{x} - D\omega) = \dot{\mathbf{x}} - (\dot{D}\omega + D\dot{\omega})$, and

$$\begin{aligned} \dot{T}(\mathbf{x}_0, \mathbf{x}) &= \frac{\partial}{\partial t} \exp\left(-\int_0^D \sigma_t(\mathbf{x}'') d\tau'\right) \\ &= -T(\mathbf{x}_0, \mathbf{x}) \frac{\partial}{\partial t} \int_0^D \sigma_t(\mathbf{x}'') d\tau' \\ &= -T(\mathbf{x}_0, \mathbf{x}) (\Sigma_t(\mathbf{x}, \omega, D) + \dot{D} \sigma_t(\mathbf{x}_0)), \end{aligned} \quad (36)$$

where $\mathbf{x}'' := \mathbf{x} - \tau'\omega$, and Σ_t follows the definition in Eq. (23). Compared to $T(\mathbf{x}', \mathbf{x})$ given by Eq. (22), $T(\mathbf{x}_0, \mathbf{x})$ has one more term $\dot{D} \sigma_t(\mathbf{x}_0)$ since D is generally time-varying while τ is not.

Recall that $(\mathcal{K}_S L)(\mathbf{x}, \omega) = T(\mathbf{x}_0, \omega) L_s^c(\mathbf{x}_0, \omega)$. Provided Eq. (36), it follows that

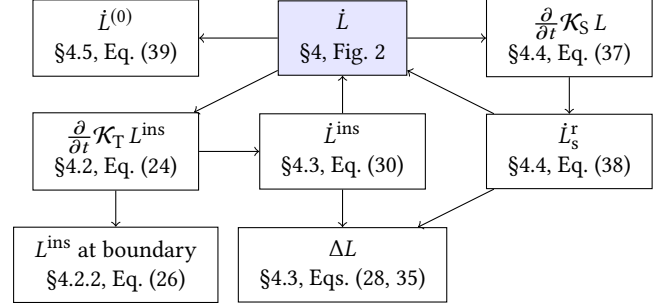


Fig. 6. A summary of dependencies between \dot{L} -related quantities derived in §4. In this figure, an arrow from A to B indicates that A depends on B. The cycles in this diagram indicate that the whole system effectively forms a transport equation of \dot{L} , as previously showed by the DRTE (18).

$$\begin{aligned} \left(\frac{\partial}{\partial t} \mathcal{K}_S L\right)(\mathbf{x}, \omega) &= \frac{\partial}{\partial t} [T(\mathbf{x}_0, \mathbf{x}) L_s^r(\mathbf{x}_0, \mathbf{x})] \\ &= T(\mathbf{x}_0, \omega) \dot{L}_s^r(\mathbf{x}_0, \omega) + \dot{T}(\mathbf{x}_0, \omega) L_s^r(\mathbf{x}_0, \omega) \\ &= T(\mathbf{x}_0, \omega) [\dot{L}_s^r(\mathbf{x}_0, \omega) - (\Sigma_t(\mathbf{x}, \omega, D) + \dot{D} \sigma_t(\mathbf{x}_0)) L_s^r(\mathbf{x}_0, \omega)], \end{aligned} \quad (37)$$

where

$$\begin{aligned} \dot{L}_s^r(\mathbf{x}, \omega) &= \int_{\mathbb{S}^2} f_s(\mathbf{x}, -\omega', \omega) \dot{L}(\mathbf{x}, \omega') d\omega' \\ &\quad + \int_{\mathbb{S}^2} \dot{f}_s(\mathbf{x}, -\omega', \omega) L(\mathbf{x}, \omega') d\omega' \\ &\quad + \int_{\partial\Omega(\mathbf{x})} \left| \left\langle \mathbf{n}, \frac{\partial}{\partial t}(\mathbf{y} \rightarrow \mathbf{x}) \right\rangle \right| f_s(\mathbf{x}, \mathbf{x} \rightarrow \mathbf{y}, \omega) \\ &\quad \Delta L(\mathbf{x}, \mathbf{y} \rightarrow \mathbf{x}) V(\mathbf{x}, \mathbf{y}) \frac{\sin \theta}{\|\mathbf{y} - \mathbf{x}\|} d\ell(\mathbf{y}). \end{aligned} \quad (38)$$

In Eq. (38), ΔL follows Eqs. (28, 35), and \dot{f}_s can generally be obtained using symbolic/automated differentiation, analogous to \dot{f}_p . At a high level, the first term on the RHS of Eq. (38) corresponds to the \mathcal{K} operator in the DRTE (18) while the others to \mathcal{K}_0 .

4.5 Completing \dot{L}

The last term $\dot{L}^{(0)}$ in Figure 2, which acts as the source term of the DRTE (18), equals

$$\begin{aligned} \dot{L}^{(0)}(\mathbf{x}, \omega) &= \frac{\partial}{\partial t} [T(\mathbf{x}_0, \mathbf{x}) L_s^c(\mathbf{x}_0, \omega)] \\ &= T(\mathbf{x}_0, \mathbf{x}) \dot{L}_s^c(\mathbf{x}_0, \omega) + \dot{T}(\mathbf{x}_0, \mathbf{x}) L_s^c(\mathbf{x}_0, \omega) \\ &= T(\mathbf{x}_0, \mathbf{x}) [\dot{L}_s^c(\mathbf{x}_0, \omega) - (\Sigma_t(\mathbf{x}, \omega, D) + \dot{D} \sigma_t(\mathbf{x}_0)) L_s^c(\mathbf{x}_0, \omega)], \end{aligned} \quad (39)$$

Similar to \dot{f}_p and \dot{f}_s , $\dot{L}_s^c(\mathbf{x}_0, \omega)$ can be nonzero and obtained using symbolic/automated differentiation.

Putting together. Combining (i) Eq. (24) in §4.2 that differentiates \mathcal{K}_T , (ii) Eq. (30) in §4.3 that handles \mathcal{K}_C , (iii) Eqs. (37, 38) in §4.4 that

differentiate \mathcal{K}_S , and (iv) Eq. (39) above that differentiates $L^{(0)}$ completes our derivation of \dot{L} outlined in Figure. (2). Figure 6 illustrates the dependencies between the previously derived quantities.

Homogeneous Media. Our previous derivations enjoy the generality for handling media with spatially varying radiative transfer parameters σ_t , σ_s , and f_p .

On the other hand, for homogeneous media with spatially (and temporally) invariant parameters, the time derivatives of interior and in-scattered radiances simplify considerably:

$$\dot{L}(\mathbf{x}, \omega) = \int_0^D e^{-\sigma_t \tau} \sigma_s \dot{L}^{\text{ins}}(\mathbf{x}', \omega) d\tau + e^{-\sigma_t D} \left[\dot{L}_s(\mathbf{x}_0, \omega) + \dot{D} \left(\sigma_s L^{\text{ins}}(\mathbf{x}_0, \omega) - \sigma_t L_s(\mathbf{x}_0, \omega) \right) \right], \quad (40)$$

$$\begin{aligned} \dot{L}^{\text{ins}}(\mathbf{x}, \omega) = & \int_{\mathbb{S}^2} f_p(-\omega', \omega) \dot{L}(\mathbf{x}, \omega') d\omega' + \int_{\mathbb{S}^2} \dot{f}_p(-\omega', \omega) L(\mathbf{x}, \omega') d\omega' + \\ & \int_{\partial\Omega(\mathbf{x})} \left| \left\langle \mathbf{n}, \frac{\partial}{\partial t}(\mathbf{y} \rightarrow \mathbf{x}) \right\rangle \right| f_p(\mathbf{x} \rightarrow \mathbf{y}, \omega) \Delta L(\mathbf{x}, \mathbf{y} \rightarrow \mathbf{x}) V(\mathbf{x}, \mathbf{y}) \frac{\sin \theta}{\|\mathbf{y} - \mathbf{x}\|} d\ell(\mathbf{y}). \end{aligned} \quad (41)$$

$$\dot{L}^{(0)}(\mathbf{x}, \omega) = e^{-\sigma_t D} \left[\dot{L}_s^e(\mathbf{x}_0, \omega) - \dot{D} \sigma_t L_s^e(\mathbf{x}_0, \omega) \right]. \quad (42)$$

We introduce Monte Carlo estimators for homogeneous media based on Eqs. (40, 41) in §5 and discuss generalizations to heterogeneous media in §6.2.

4.6 Differentiating Pixel Intensities

In physically based rendering, the intensity of each pixel is typically modeled as the inner product between the incident radiance L_s^i and some (normalized) reconstruction kernel K over the pixel footprint \mathcal{P} on the image plane:

$$I = \int_{\mathcal{P}} L(\mathbf{x}, \omega(\mathbf{x})) K(\mathbf{x}) d\mathbf{x}, \quad (43)$$

where the exact form of $\omega(\mathbf{x})$ depends on the camera model. A perspective camera with projection center \mathbf{x}^{cam} , for instance, has $\omega(\mathbf{x}) = \mathbf{x} \rightarrow \mathbf{x}^{\text{cam}}$.

When K is time-invariant and continuous in \mathbf{x} , Eq. (43) can be differentiated via

$$\begin{aligned} \dot{I} = & \int_{\mathcal{P}} \dot{L}(\mathbf{x}, \omega(\mathbf{x})) K(\mathbf{x}) d\mathbf{x} \\ & + \int_{\partial\mathcal{P}} |\langle \mathbf{n}, \mathbf{v} \rangle| \Delta L(\mathbf{x}, \omega(\mathbf{x})) K(\mathbf{x}) d\ell(\mathbf{x}), \end{aligned} \quad (44)$$

where $\partial\mathcal{P}$ denotes all discontinuities of $L(\mathbf{x}, \omega(\mathbf{x}))$, and \mathbf{n}, \mathbf{v} capture the image-plane normal and velocity of these discontinuities.

Notice that, when the camera's location or orientation is time-varying (which is required for optimizing camera pose), so be the corresponding \mathbf{x} and $\omega(\mathbf{x})$ in Eqs. (43, 44). This is why our derivations of \dot{L} in the previous subsections allow both \mathbf{x} and ω to be time-varying.

5 UNBIASED MONTE CARLO ESTIMATORS

In this section, we aim to introduce an unbiased Monte Carlo estimator for the time derivatives of the interior radiance \dot{L} . To simplify the derivations, we focus on *homogeneous media* based on time derivatives expressed in §4.5. We discuss how our method can be extended to support heterogeneous media in §6.2.

Specifically, we build a Monte Carlo estimator analogous to path tracing with next-event estimation (NEE). Let

$$L^{(1)} := L - L^{(0)} = (\mathcal{K}_T \mathcal{K}_C + \mathcal{K}_S) L. \quad (45)$$

Then, for homogeneous media, $\dot{L}^{(1)}$ can be obtained by subtracting $\dot{L}^{(0)}$ given by Eq. (42) from \dot{L} provided by Eq. (40), leading to

$$\begin{aligned} \dot{L}^{(1)}(\mathbf{x}, \omega) = & \int_0^D e^{-\sigma_t \tau} \sigma_s \dot{L}^{\text{ins}}(\mathbf{x}', \omega) d\tau \\ & + e^{-\sigma_t D} \left[\dot{L}_s^i(\mathbf{x}_0, \omega) + \dot{D} \left(\sigma_s L^{\text{ins}}(\mathbf{x}_0, \omega) - \sigma_t L_s^i(\mathbf{x}_0, \omega) \right) \right]. \end{aligned} \quad (46)$$

Based on the decomposition of $\dot{L} = \dot{L}^{(1)} + \dot{L}^{(0)}$, we can rewrite Eqs. (38, 41) as

$$\begin{aligned} \dot{L}_s^i(\mathbf{x}, \omega) = & \int_{\mathbb{S}^2} f_s(\mathbf{x}, -\omega', \omega) \dot{L}^{(1)}(\mathbf{x}, \omega') d\omega' + \int_{\mathbb{S}^2} f_s(\mathbf{x}, -\omega', \omega) \dot{L}^{(0)}(\mathbf{x}, \omega') d\omega' + \\ & \int_{\mathbb{S}^2} \dot{f}_s(\mathbf{x}, -\omega', \omega) L(\mathbf{x}, \omega') d\omega' + \int_{\partial\Omega(\mathbf{x})} \left| \left\langle \mathbf{n}, \frac{\partial}{\partial t}(\mathbf{y} \rightarrow \mathbf{x}) \right\rangle \right| f_s(\mathbf{x}, \mathbf{x} \rightarrow \mathbf{y}, \omega) \Delta L(\mathbf{x}, \mathbf{y} \rightarrow \mathbf{x}) V(\mathbf{x}, \mathbf{y}) \frac{\sin \theta}{\|\mathbf{y} - \mathbf{x}\|} d\ell(\mathbf{y}), \end{aligned} \quad (47)$$

$$\begin{aligned} \dot{L}^{\text{ins}}(\mathbf{x}, \omega) = & \int_{\mathbb{S}^2} f_p(-\omega', \omega) \dot{L}^{(1)}(\mathbf{x}, \omega') d\omega' + \int_{\mathbb{S}^2} f_p(-\omega', \omega) \dot{L}^{(0)}(\mathbf{x}, \omega') d\omega' + \\ & \int_{\mathbb{S}^2} \dot{f}_p(-\omega', \omega) L(\mathbf{x}, \omega') d\omega' + \int_{\partial\Omega(\mathbf{x})} \left| \left\langle \mathbf{n}, \frac{\partial}{\partial t}(\mathbf{y} \rightarrow \mathbf{x}) \right\rangle \right| f_p(\mathbf{x} \rightarrow \mathbf{y}, \omega) \Delta L(\mathbf{x}, \mathbf{y} \rightarrow \mathbf{x}) V(\mathbf{x}, \mathbf{y}) \frac{\sin \theta}{\|\mathbf{y} - \mathbf{x}\|} d\ell(\mathbf{y}). \end{aligned} \quad (48)$$

Since $\dot{L}^{(0)}$ only involves known quantities, the integrals on $\dot{L}^{(0)}$ in Eqs. (47, 48) can be estimated directly. Similar to conventional path tracing, this can be done using light source and phase function/BSDF samplings combined with MIS.

Algorithm 1 provides the pseudocode of an unbiased Monte Carlo estimator of \dot{L} based on Eqs. (46–48). Algorithms 2 and 3 outline how ΔL and L^{ins} , two key ingredients of \dot{L} , can be estimated based on Eq. (35) as well as Eqs. (5, 26).

[TODO: Go over Algorithm 1 in text.]

6 GENERALIZATIONS

Recall that our derivations in §4 and §5 rely on a few simplifying assumptions:

Algorithm 1 Unbiased Monte Carlo estimator of \dot{L}

```

1: function  $\dot{L}(\mathbf{x}, \dot{\mathbf{x}}, \boldsymbol{\omega}, \dot{\boldsymbol{\omega}})$ 
2:   Calculate  $D$  and  $\dot{D}$  based on  $\mathbf{x}, \dot{\mathbf{x}}, \boldsymbol{\omega}$ , and  $\dot{\boldsymbol{\omega}}$   $\triangleright$  Appendix B
3:    $\dot{L} \leftarrow \dot{L}^{(0)}(\mathbf{x}, \dot{\mathbf{x}}, \boldsymbol{\omega})$   $\triangleright$  (39)
4:    $\mathcal{T}_{\text{path}} \leftarrow 1$   $\triangleright$  path throughput
5:   while true do
6:      $\tau \leftarrow -\log(\text{rand}())/\sigma_t$ 
7:     if  $\tau < D$  then
8:        $\mathbf{x} \leftarrow \mathbf{x} - \tau\boldsymbol{\omega}$   $\triangleright \mathbf{x} \in \Omega \setminus \partial\Omega$ 
9:        $\dot{\mathbf{x}} \leftarrow \dot{\mathbf{x}} - \tau\dot{\boldsymbol{\omega}}$ 
10:       $\mathcal{T}_{\text{path}} \leftarrow \mathcal{T}_{\text{path}}(\sigma_s/\sigma_t)$ 
11:      Estimate  $v_0 = \int_{\mathbb{S}^2} f_p(-\boldsymbol{\omega}', \boldsymbol{\omega}) \dot{L}^{(0)}(\mathbf{x}, \boldsymbol{\omega}') d\boldsymbol{\omega}'$ 
12:      if  $\|\dot{\boldsymbol{\omega}}\| > 0$  then
13:        Estimate  $v_1 = \int_{\mathbb{S}^2} \dot{f}_p(-\boldsymbol{\omega}', \boldsymbol{\omega}) L(\mathbf{x}, \boldsymbol{\omega}') d\boldsymbol{\omega}'$ 
14:      else
15:         $v_1 \leftarrow 0$ 
16:      end if
17:      Draw  $\mathbf{y}$  from  $\partial\Omega(\mathbf{x})$  with probability  $p(\mathbf{y})$ 
18:       $\boldsymbol{\omega}' \leftarrow (\mathbf{y} \rightarrow \mathbf{x})$ 
19:      Calculate  $\mathbf{n}, \dot{\boldsymbol{\omega}}'$  using Eqs. (31, 32)
20:       $\Delta L \leftarrow \Delta L(\mathbf{x}, \dot{\mathbf{x}}, \boldsymbol{\omega}', \dot{\boldsymbol{\omega}}')$   $\triangleright$  Alg. 2
21:       $v_2 \leftarrow |\langle \mathbf{n}, \dot{\boldsymbol{\omega}}' \rangle| f_p(-\boldsymbol{\omega}', \boldsymbol{\omega}) \Delta L \frac{V(\mathbf{x}, \mathbf{y}) \sin \theta}{\|\mathbf{y} - \mathbf{x}\| p(\mathbf{y})}$ 
22:       $\dot{L} \leftarrow \dot{L} + (v_0 + v_1 + v_2) \mathcal{T}_{\text{path}}$ 
23:      Draw  $\boldsymbol{\omega}' \sim f_p(-\boldsymbol{\omega}', \boldsymbol{\omega})$ 
24:       $\boldsymbol{\omega} \leftarrow \boldsymbol{\omega}', \dot{\boldsymbol{\omega}} \leftarrow 0$ 
25:    else
26:       $\mathbf{x} \leftarrow \mathbf{x} - D\boldsymbol{\omega}$   $\triangleright \mathbf{x} \in \partial\Omega$ 
27:       $\dot{\mathbf{x}} \leftarrow \dot{\mathbf{x}} - \dot{D}\boldsymbol{\omega} - D\dot{\boldsymbol{\omega}}$ 
28:      Estimate  $v_0 = \int_{\mathbb{S}^2} f_s(\mathbf{x}, -\boldsymbol{\omega}', \boldsymbol{\omega}) \dot{L}^{(0)}(\mathbf{x}, \boldsymbol{\omega}') d\boldsymbol{\omega}'$ 
29:      Estimate  $v_1 = \int_{\mathbb{S}^2} \dot{f}_s(\mathbf{x}, -\boldsymbol{\omega}', \boldsymbol{\omega}) L(\mathbf{x}, \boldsymbol{\omega}') d\boldsymbol{\omega}'$ 
30:      Draw  $\mathbf{y}$  from  $\partial\Omega(\mathbf{x})$  with probability  $p(\mathbf{y})$ 
31:       $\boldsymbol{\omega}' \leftarrow (\mathbf{y} \rightarrow \mathbf{x})$ 
32:      Calculate  $\mathbf{n}, \dot{\boldsymbol{\omega}}'$  using Eqs. (31, 32)
33:       $\Delta L \leftarrow \Delta L(\mathbf{x}, \dot{\mathbf{x}}, \boldsymbol{\omega}', \dot{\boldsymbol{\omega}}')$   $\triangleright$  Alg. 2
34:       $v_2 \leftarrow |\langle \mathbf{n}, \dot{\boldsymbol{\omega}}' \rangle| f_s(\mathbf{x}, -\boldsymbol{\omega}', \boldsymbol{\omega}) \Delta L \frac{V(\mathbf{x}, \mathbf{y}) \sin \theta}{\|\mathbf{y} - \mathbf{x}\| p(\mathbf{y})}$ 
35:      Estimate  $L^{\text{ins}} = L^{\text{ins}}(\mathbf{x}, \boldsymbol{\omega})$   $\triangleright$  Alg. 3
36:      Estimate  $L_s^{\text{r}} = L_s^{\text{r}}(\mathbf{x}, \boldsymbol{\omega})$ 
37:       $\dot{L} \leftarrow \dot{L} + [v_0 + v_1 + v_2 + \dot{D}(\sigma_s L^{\text{ins}} - \sigma_t L_s^{\text{r}})] \mathcal{T}_{\text{path}}$ 
38:      Draw  $\boldsymbol{\omega}'$  with probability  $p(\boldsymbol{\omega}')$ 
39:       $\mathcal{T}_{\text{path}} \leftarrow \mathcal{T}_{\text{path}}(f_s(\mathbf{x}, -\boldsymbol{\omega}', \boldsymbol{\omega})/p(\boldsymbol{\omega}'))$ 
40:       $\boldsymbol{\omega} \leftarrow \boldsymbol{\omega}', \dot{\boldsymbol{\omega}} \leftarrow 0$ 
41:    end if
42:    Calculate  $D$  and  $\dot{D}$  based on  $\mathbf{x}, \dot{\mathbf{x}}, \boldsymbol{\omega}$ , and  $\dot{\boldsymbol{\omega}}$ 
43:  end while
44:  return  $\dot{L}$ 
45: end function

```

- There is no delta light source or perfectly specular surface;
- All material parameters are continuous and time-independent;
- All scene geometries are depicted using polygonal meshes.

We now discuss possible generalizations of our previous derivations by relaxing some of these assumptions.

Algorithm 2 Unbiased Monte Carlo estimator of ΔL

```

1: function  $\Delta L(\mathbf{x}, \dot{\mathbf{x}}, \boldsymbol{\omega}, \dot{\boldsymbol{\omega}})$ 
2:   Calculate  $D^-$  and  $D^+$  based on  $\mathbf{x}, \dot{\mathbf{x}}, \boldsymbol{\omega}$ , and  $\dot{\boldsymbol{\omega}}$   $\triangleright$  Eq. (33)
3:    $\mathbf{x}^- \leftarrow \mathbf{x} - D^- \boldsymbol{\omega}, \mathbf{x}^+ \leftarrow \mathbf{x} - D^+ \boldsymbol{\omega}$ 
4:   Estimate  $L_s^- = L_s(\mathbf{x}^-, \boldsymbol{\omega})$  and  $L_s^+ = L_s(\mathbf{x}^+, \boldsymbol{\omega})$ 
5:    $\Delta L \leftarrow T(\mathbf{x}^-, \mathbf{x}) L_s^- - T(\mathbf{x}^+, \mathbf{x}) L_s^+$ 
6:    $D_0 \leftarrow \min(D^-, D^+)$ 
7:    $\tau \leftarrow D_0 - \log(\text{rand}())/\sigma_t$ 
8:   if  $\tau < \max(D^-, D^+)$  then
9:      $\mathbf{x}' \leftarrow \mathbf{x} - \tau\boldsymbol{\omega}$ 
10:     $v \leftarrow T(\mathbf{x}, \mathbf{x} - D_0 \boldsymbol{\omega}) \frac{\sigma_s(\mathbf{x}')}{\sigma_t(\mathbf{x}')} L^{\text{ins}}(\mathbf{x}', \boldsymbol{\omega})$ 
11:    if  $D^+ < D^-$  then
12:       $\Delta L \leftarrow \Delta L + v$ 
13:    else
14:       $\Delta L \leftarrow \Delta L - v$ 
15:    end if
16:  end if
17:  return  $\Delta L$ 
18: end function

```

6.1 Point Light Sources

We now discuss how our derivations in §4 can be extended to support point sources. Other delta light sources (e.g., directional) can be handled in a similar manner.

For a uniform point source located at $\mathbf{x}^{\text{light}}$ with intensity I^{light} , L^{ins} becomes

$$L^{\text{ins}}(\mathbf{x}, \boldsymbol{\omega}) = \int_{\mathbb{S}^2} f_p(\mathbf{x}, -\boldsymbol{\omega}', \boldsymbol{\omega}) L^{(1)}(\mathbf{x}, \boldsymbol{\omega}') d\boldsymbol{\omega}' + \frac{V(\mathbf{x}, \mathbf{x}^{\text{light}}) T(\mathbf{x}, \mathbf{x}^{\text{light}}) f_p(\mathbf{x}, \mathbf{x} \rightarrow \mathbf{x}^{\text{light}}, \boldsymbol{\omega}) I^{\text{light}}}{\|\mathbf{x} - \mathbf{x}^{\text{light}}\|^2}. \quad (49)$$

Recall that, according to Eq. (46), $L^{(1)}(\mathbf{x}, \boldsymbol{\omega})$ involves an integral of L^{ins} over a straight line. When L^{ins} takes the form of Eq. (49), it can have jump discontinuities along this line due to the sudden changes in visibility V . In other words, when a straight line goes across hard volumetric shadow boundaries resulting from delta light sources, L^{ins} will be discontinuous at the line-shadow intersections.

Algorithm 3 Unbiased Monte Carlo estimator of L^{ins}

```

1: function  $L^{\text{ins}}(\mathbf{x}, \boldsymbol{\omega})$ 
2:   Draw  $\boldsymbol{\omega}' \sim f_p(-\boldsymbol{\omega}', \boldsymbol{\omega})$ 
3:   if  $\mathbf{x} \in \partial\Omega$  then
4:     if  $\langle \mathbf{n}(\mathbf{x}), \boldsymbol{\omega}' \rangle > 0$  then
5:       Estimate  $L^{\text{ins}} = L(\mathbf{x}, \boldsymbol{\omega}')$ 
6:     else
7:       Estimate  $L^{\text{ins}} = L_s(\mathbf{x}, \boldsymbol{\omega}')$ 
8:     end if
9:   else
10:    Estimate  $L^{\text{ins}} = L(\mathbf{x}, \boldsymbol{\omega}')$ 
11:   end if
12:   return  $L^{\text{ins}}$ 
13: end function

```

Given $\mathbf{x} \in \Omega \setminus \partial\Omega$ and $\omega \in \mathbb{S}^2$, let $\Gamma(\mathbf{x}, \omega) \subset (0, D)$ to contain all discontinuous locations of $V(\mathbf{x} - \tau\omega, \mathbf{x}^{\text{light}})$ for $0 < \tau < D$. Then, according to Corollary 2, we have

$$\begin{aligned} \left(\frac{\partial}{\partial t} \mathcal{K}_T L^{\text{ins}}\right)(\mathbf{x}, \omega) &= \int_0^D T(\mathbf{x}', \mathbf{x}) \sigma_s(\mathbf{x}') \dot{L}^{\text{ins}}(\mathbf{x}', \omega) d\tau \\ &+ \int_0^D T(\mathbf{x}', \mathbf{x}) (\dot{\sigma}_s(\mathbf{x}') - \Sigma_t(\mathbf{x}, \omega, \tau) \sigma_s(\mathbf{x}')) L^{\text{ins}}(\mathbf{x}', \omega) d\tau \\ &+ \dot{D} T(\mathbf{x}_0, \mathbf{x}) \sigma_s(\mathbf{x}_0) L^{\text{ins}}(\mathbf{x}_0, \omega), \\ &+ \sum_{\tau \in \Gamma(\mathbf{x}, \omega)} |\dot{\tau}| T(\mathbf{x}', \mathbf{x}) \sigma_s(\mathbf{x}') \Delta L^{\text{ins}}(\mathbf{x}', \omega), \end{aligned} \quad (50)$$

where $\mathbf{x}' := \mathbf{x} - \tau\omega$, and

$$\begin{aligned} \Delta L^{\text{ins}}(\mathbf{x}', \omega) &= \lim_{\epsilon \rightarrow 0^-} L^{\text{ins}}(\mathbf{x}' + \epsilon(\dot{\mathbf{x}}' - \dot{\tau}\omega - \tau\dot{\omega}), \omega + \epsilon\dot{\omega}) \\ &- \lim_{\epsilon \rightarrow 0^+} L^{\text{ins}}(\mathbf{x}' + \epsilon(\dot{\mathbf{x}}' - \dot{\tau}\omega - \tau\dot{\omega}), \omega + \epsilon\dot{\omega}). \end{aligned} \quad (51)$$

In general, similar to \dot{D} , the exact form of $\dot{\tau}$ depends on $\dot{\mathbf{x}}$ and the time-varying scene geometry. When the shadow boundary is created by a point light source and a straight edge, $\dot{\tau}$ takes identical forms as \dot{D} given by Eqs. (81, 82).

6.2 Heterogeneity

TBD.

7 GRADIENT-BASED OPTIMIZATION OF SCENE GEOMETRY

TBD.

8 RESULTS

We implemented Algorithms 1, 2, and 3 outlined in §5 in C++ using the Embree ray tracer. Additionally, we created a few standalone implementations to demonstrate our generalized derivations (§6).

8.1 Validation and Evaluation

Validation. TBD

Performance. TBD

8.2 Main Results

TBD

8.3 Generalizations

Point light source. TBD

Heterogeneous medium. TBD

Higher-order surface. TBD

8.4 Limitations and Future Work

TBD.

9 CONCLUSION

TBD.

REFERENCES

- Subrahmanyan Chandrasekhar. 2013. *Radiative transfer*. Courier Corporation.
- Harley Flanders. 1973. Differentiation under the integral sign. *The American Mathematical Monthly* 80, 6 (1973), 615–627.
- L Gary Leal. 2007. *Advanced Transport Phenomena: fluid mechanics and convective transport processes*. Vol. 7. Cambridge University Press.
- Tzu-Mao Li, Miika Aittala, Frédo Durand, and Jaakko Lehtinen. 2018. Differentiable Monte Carlo ray tracing through edge sampling. *ACM Trans. Graph.* 37, 6 (2018), 222:1–222:11.
- Shuang Zhao, Frédo Durand, and Changxi Zheng. 2018. Inverse diffusion curves using shape optimization. *IEEE transactions on visualization and computer graphics* 24, 7 (2018), 2153–2166.

A EXAMPLES

Example 1. Let $\Omega(r) := \{\mathbf{x} \in \mathbb{R}^2 : \|\mathbf{x}\| \leq r\}$ be a 2D disc centered at the origin with radius r and

$$I(r) := \int_{\Omega(r)} \frac{1}{\|\mathbf{x}\|} dA(\mathbf{x}), \quad (52)$$

where dA denotes the area measure. In this case, the boundary is simply the circumference of the disc: $\partial\Omega(r) = \{\mathbf{x} \in \mathbb{R}^2 : \|\mathbf{x}\| = r\}$. Then, since the integrand $1/\|\mathbf{x}\|$ does not depend on r , according to Theorem 1, it holds that

$$\begin{aligned} \left(\frac{\partial}{\partial r} I\right)(r) &= \int_{\partial\Omega(r)} \frac{\langle \mathbf{n}(\mathbf{x}), \mathbf{v}(\mathbf{x}) \rangle}{\|\mathbf{x}\|} d\ell(\mathbf{x}) \\ &= \int_{\partial\Omega(r)} \frac{\langle \mathbf{n}(\mathbf{x}), \mathbf{v}(\mathbf{x}) \rangle}{r} d\ell(\mathbf{x}), \end{aligned} \quad (53)$$

where $d\ell$ denotes the curve length measure. Based on the parameterization of Ω , it holds that the normal velocity $\langle \mathbf{n}(\mathbf{x}), \mathbf{v}(\mathbf{x}) \rangle$ on any point \mathbf{x} on its boundary $\partial\Omega$ equals one constantly. Thus, Eq. (53) becomes

$$\left(\frac{\partial}{\partial r} I\right)(r) = \int_{\partial\Omega(r)} \frac{1}{r} d\ell(\mathbf{x}) = 2\pi r \cdot \frac{1}{r} \equiv 2\pi, \quad (54)$$

which agrees with the result obtained by directly differentiating Eq. (52). Specifically, it can be shown that $I(r) = 2\pi r$, yielding $\left(\frac{\partial}{\partial r} I\right)(r) \equiv 2\pi$.

Example 2. We now alter the first example by making the integrand to depend on r :

$$I(r) := \int_{\Omega(r)} \frac{r}{\|\mathbf{x}\|} dA(\mathbf{x}). \quad (55)$$

Then, it holds that $I(r) = 2\pi r^2$. Since $\frac{\partial}{\partial r}(r/\|\mathbf{x}\|) = 1/\|\mathbf{x}\|$, we have

$$\left(\frac{\partial}{\partial r} I\right)(r) = \underbrace{\int_{\Omega(r)} \frac{1}{\|\mathbf{x}\|} dA(\mathbf{x})}_{= 2\pi r} + \underbrace{\int_{\partial\Omega(r)} d\ell(\mathbf{x})}_{= 2\pi r} = 4\pi r, \quad (56)$$

which agrees with $\left(\frac{\partial}{\partial r} I\right)(r) = \frac{\partial}{\partial r}(2\pi r^2) = 4\pi r$.

Example 3. We now extend the previous example to 3D by letting $\Omega(r) := \{\mathbf{x} \in \mathbb{R}^3 : \|\mathbf{x}\| \leq r\}$, $\partial\Omega(r) = \{\mathbf{x} \in \mathbb{R}^3 : \|\mathbf{x}\| = r\}$, and

$$I(r) := \int_{\Omega(r)} \frac{r}{\|\mathbf{x}\|^2} dV(\mathbf{x}), \quad (57)$$

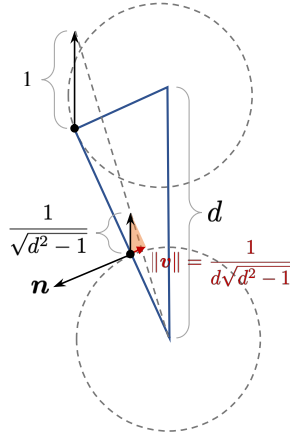


Fig. 7. Calculating the projected velocity for Example 5.

where dV denotes the volume measure. Then, it holds that $I(r) = 4\pi r^2$. As $\frac{\partial}{\partial r}(r/\|\mathbf{x}\|^2) = \|\mathbf{x}\|^{-2}$,

$$\left(\frac{\partial}{\partial r}I\right)(r) = \underbrace{\int_{\Omega(r)} \frac{1}{\|\mathbf{x}\|^2} dV(\mathbf{x})}_{= 4\pi r} + \underbrace{\int_{\partial\Omega(r)} \frac{1}{r} dA(\mathbf{x})}_{= 4\pi r} = 8\pi r, \quad (58)$$

which agrees with the direct differentiation of $I(r)$.

Example 4. We now consider an example where the integrand is discontinuous on the boundary. Specifically, for all $\mathbf{x} \in \mathbb{R}^3$, let

$$f(\mathbf{x} | r) = \begin{cases} 1 & \|\mathbf{x}\| < r, \\ \text{undefined} & \|\mathbf{x}\| \geq r. \end{cases} \quad (59)$$

Note that, although f is undefined when $\|\mathbf{x}\| = r$, it remains integrable over $\Omega(r)$ under the volume measure. Let

$$I(r) = \int_{\Omega(r)} f(\mathbf{x} | r) dV(\mathbf{x}). \quad (60)$$

It is easy to verify that $I(r) = \frac{4}{3}\pi r^3$. Differentiating Eq. (60) using Corollary 2 yields

$$\left(\frac{\partial}{\partial r}I\right)(r) = \int_{\Gamma(r)} \underbrace{\lim_{\epsilon \rightarrow 0^+} f(\mathbf{x} + \epsilon \mathbf{v}(\mathbf{x}) | r)}_{= 1} dA(\mathbf{x}) = 4\pi r^2, \quad (61)$$

which agrees with direct differentiation of I as $\frac{\partial}{\partial r}\left(\frac{4}{3}\pi r^3\right) = 4\pi r^2$.

Example 5. In this example, we consider the derivative of the solid angle (viewed from the origin) subtended by a unit-radius sphere centered at $(0, 0, d)$ with $d > 1$. Let Ω be the projection of the sphere on \mathbb{S}^2 , which is a spherical cap, then the solid angle equals the surface area of Ω given by

$$I(d) = \int_{\Omega(d)} dA(\omega). \quad (62)$$

According to Theorem 1, differentiating Eq. (62) leads to

$$\left(\frac{\partial}{\partial d}I\right)(d) = \int_{\partial\Omega(d)} \langle \mathbf{n}(\omega), \mathbf{v}(\omega) \rangle d\ell(\omega), \quad (63)$$

where $\mathbf{n}(\omega)$ and $\mathbf{v}(\omega)$ are the normal and velocity of the boundary $\partial\Omega$ at ω , respectively. Note that both $\mathbf{n}(\omega)$ and $\mathbf{v}(\omega)$ lie within the tangent plane at ω . As shown in the Figure 7, it holds that $\langle \mathbf{n}(\omega), \mathbf{v}(\omega) \rangle \equiv -1/(d\sqrt{d^2 - 1})$ for all $\omega \in \partial\Omega(d)$. Thus,

$$\left(\frac{\partial}{\partial d}I\right)(d) = -\frac{2\pi}{d^2\sqrt{d^2 - 1}}. \quad (64)$$

On the other hand, we know that $I(d) = 2\pi(1 - \sqrt{1 - (1/d)^2})$. Differentiating this symbolically yields the same answer as Eq. (64).

B DERIVATIONS OF \dot{D} FOR SPECIFIC SHAPES

In this section, we provide derivations of \dot{D} from Eqs. (20–24) for a few specific geometric shapes and velocities.

B.1 Planar Surfaces

We start with deriving \dot{D} for *piecewise-planar geometries* (e.g., polygonal meshes).

Translation. Consider a plane that is given by $\{\mathbf{y} : \langle \mathbf{n}, \mathbf{y} \rangle = \langle \mathbf{n}, \mathbf{p} \rangle\}$ at $t = 0$ and translates under spatially and temporally invariant velocity \mathbf{v} . Then, at time t , the plane equation becomes

$$\langle \mathbf{n}, \mathbf{y} \rangle = \langle \mathbf{n}, \mathbf{p} \rangle + \langle \mathbf{n}, \mathbf{v} \rangle t. \quad (65)$$

Then, substituting \mathbf{y} with the ray equation with *time-varying* origin \mathbf{x} and *time-independent* direction ω gives

$$\langle \mathbf{n}, \mathbf{x} - d\omega \rangle = \langle \mathbf{n}, \mathbf{p} \rangle + \langle \mathbf{n}, \mathbf{v} \rangle t, \quad (66)$$

which in turn leads to

$$D(t) = \frac{\langle \mathbf{n}, \mathbf{x} - \mathbf{p} - t\mathbf{v} \rangle}{\langle \mathbf{n}, \omega \rangle}. \quad (67)$$

Lastly, \dot{D} can be obtained by differentiating Eq. (67). When \mathbf{x} and ω are both time-varying,

$$\dot{D} = \frac{\partial}{\partial t} D \Big|_{t=0} = \frac{\langle \mathbf{n}, \dot{\mathbf{x}} - \mathbf{v} \rangle \langle \mathbf{n}, \omega \rangle - \langle \mathbf{n}, \mathbf{x} - \mathbf{p} \rangle \langle \mathbf{n}, \dot{\omega} \rangle}{\langle \mathbf{n}, \omega \rangle^2}, \quad (68)$$

where $\dot{\mathbf{x}}$ and $\dot{\omega}$ denotes the time derivative of \mathbf{x} and ω (at time $t = 0$).

Linear transformation. Consider a plane transformed linearly via some matrix $M(t) \in \mathbb{R}^{3 \times 3}$ such that M is continuous in t and $M(0)$ equals the identity matrix. Then, the plane at time t becomes

$$\{M(t)\mathbf{y} : \mathbf{n}^\top M^{-1}(t)M(t)\mathbf{y} = \mathbf{n}^\top M^{-1}(t)M(t)\mathbf{p}\}. \quad (69)$$

Let $\mathbf{y}' := M(t)\mathbf{y}$ and $\mathbf{m} := M^{-1}(t)\mathbf{n}$, Eq. (69) becomes

$$\{\mathbf{y}' : \langle \mathbf{m}, \mathbf{y}' \rangle = \langle \mathbf{m}, M(t)\mathbf{p} \rangle\}. \quad (70)$$

Substituting \mathbf{y}' with the ray equation gives

$$\langle \mathbf{m}, \mathbf{x} - D\omega \rangle = \langle \mathbf{m}, \mathbf{x} \rangle - \langle \mathbf{m}, \omega \rangle D = \langle \mathbf{m}, M(t)\mathbf{p} \rangle. \quad (71)$$

It follows that

$$D(t) = \frac{\langle \mathbf{m}, \mathbf{x} - M(t)\mathbf{p} \rangle}{\langle \mathbf{m}, \omega \rangle} = \frac{\langle \mathbf{n}, M^{-1}(t)\mathbf{x} - \mathbf{p} \rangle}{\langle \mathbf{n}, M^{-1}(t)\omega \rangle}. \quad (72)$$

Then,

$$\dot{D} = \frac{\langle \mathbf{n}, H\mathbf{x} + \dot{\mathbf{x}} \rangle \langle \mathbf{n}, \omega \rangle - \langle \mathbf{n}, \mathbf{x} - \mathbf{p} \rangle \langle \mathbf{n}, H\omega + \dot{\omega} \rangle}{\langle \mathbf{n}, \omega \rangle^2}, \quad (73)$$

where $H := \frac{\partial}{\partial t}(M^{-1})|_{t=0}$.

For instance, *rotations around the z-axis* can be modeled as

$$M(t) = \begin{pmatrix} \cos t & -\sin t & 0 \\ \sin t & \cos t & 0 \\ 0 & 0 & 1 \end{pmatrix}. \quad (74)$$

Then,

$$H = \left. \frac{\partial M^{-1}}{\partial t} \right|_{t=0} = \begin{pmatrix} 0 & 1 & 0 \\ -1 & 0 & 0 \\ 0 & 0 & 0 \end{pmatrix}. \quad (75)$$

In case of *uniform scaling*, we can use

$$M(t) = \begin{pmatrix} e^t & 0 & 0 \\ 0 & e^t & 0 \\ 0 & 0 & e^t \end{pmatrix}, \quad H = \begin{pmatrix} -1 & 0 & 0 \\ 0 & -1 & 0 \\ 0 & 0 & -1 \end{pmatrix}. \quad (76)$$

Similarly, for *(nonuniform) scaling along the x-axis*, we have

$$M(t) = \begin{pmatrix} e^t & 0 & 0 \\ 0 & 1 & 0 \\ 0 & 0 & 1 \end{pmatrix}, \quad H = \begin{pmatrix} -1 & 0 & 0 \\ 0 & 0 & 0 \\ 0 & 0 & 0 \end{pmatrix}. \quad (77)$$

Triangle with moving vertices. Lastly, we consider the plane determined by a triangle with time-varying vertex locations

$$\mathbf{p}(t) := (\mathbf{p}_0 + t\mathbf{v}_p), \quad \mathbf{q}(t) := (\mathbf{q}_0 + t\mathbf{v}_q), \quad \mathbf{r}(t) := (\mathbf{r}_0 + t\mathbf{v}_r). \quad (78)$$

Let $\mathbf{e}_0 := \mathbf{p}_0 - \mathbf{q}_0$, $\mathbf{e}_1 := \mathbf{r}_0 - \mathbf{q}_0$, $\Delta\mathbf{v}_0 := \mathbf{v}_p - \mathbf{v}_q$, and $\Delta\mathbf{v}_1 := \mathbf{v}_r - \mathbf{v}_q$. The plane equation at time t is

$$\langle \mathbf{n}(t), \mathbf{y} \rangle = \langle \mathbf{n}(t), \mathbf{q}(t) \rangle, \quad (79)$$

where $\mathbf{n}(t) = (\mathbf{e}_0 + t\Delta\mathbf{v}_0) \times (\mathbf{e}_1 + t\Delta\mathbf{v}_1)$. Then, substituting \mathbf{y} in Eq. (79) with the ray equation $(\mathbf{x} - D\boldsymbol{\omega})$ yields

$$D(t) = \frac{\langle \mathbf{n}(t), \mathbf{x} - \mathbf{q}(t) \rangle}{\langle \mathbf{n}(t), \boldsymbol{\omega} \rangle}, \quad (80)$$

and

$$\dot{D} = \frac{(\langle \dot{\mathbf{n}}, \Delta\mathbf{x} \rangle + \langle \mathbf{n}, \dot{\mathbf{x}} - \mathbf{v}_q \rangle) \langle \mathbf{n}, \boldsymbol{\omega} \rangle - \langle \mathbf{n}, \Delta\mathbf{x} \rangle \langle \dot{\mathbf{n}}, \boldsymbol{\omega} \rangle}{\langle \mathbf{n}, \boldsymbol{\omega} \rangle^2}, \quad (81)$$

where $\Delta\mathbf{x} := \mathbf{x}(0) - \mathbf{q}_0$, $\mathbf{n} := \mathbf{n}(0) = \mathbf{e}_0 \times \mathbf{e}_1$, and $\dot{\mathbf{n}} := \left. \frac{\partial}{\partial t} \mathbf{n} \right|_{t=0} = \Delta\mathbf{v}_0 \times \mathbf{e}_1 + \mathbf{e}_0 \times \Delta\mathbf{v}_1$. In a special case where only \mathbf{p} has nonzero velocity (i.e., $\|\mathbf{v}_p\| > 0$ and $\|\mathbf{v}_q\| = \|\mathbf{v}_r\| = 0$), Eq. (81) reduces to

$$\dot{D} = \frac{(\langle \dot{\mathbf{n}}, \Delta\mathbf{x} \rangle + \langle \mathbf{n}, \dot{\mathbf{x}} \rangle) \langle \mathbf{n}, \boldsymbol{\omega} \rangle - \langle \mathbf{n}, \Delta\mathbf{x} \rangle (\langle \dot{\mathbf{n}}, \boldsymbol{\omega} \rangle + \langle \mathbf{n}, \dot{\boldsymbol{\omega}} \rangle)}{\langle \mathbf{n}, \boldsymbol{\omega} \rangle^2}, \quad (82)$$

with $\dot{\mathbf{n}} = \mathbf{v}_p \times \mathbf{e}_1$.

B.2 Higher-Order Surfaces

§B.1 focuses on planar geometries. We now derive \dot{D} for surfaces with higher-order smoothnesses (e.g., spheres).

Sphere (translation). Consider a sphere that has radius r , is centered at the origin, and translates with time-independent velocity \mathbf{v} . Given \mathbf{x} and $\boldsymbol{\omega}$, the ray $(\mathbf{x}, -\boldsymbol{\omega})$ intersects the sphere at time t if and only if

$$\|(\mathbf{x} - t\mathbf{v}) - D\boldsymbol{\omega}\|^2 - r^2 = D^2 - 2\langle \mathbf{x} - t\mathbf{v}, \boldsymbol{\omega} \rangle D + \|\mathbf{x} - t\mathbf{v}\|^2 - r^2 = 0, \quad (83)$$

which is a quadratic equation in D . Without loss of generality, we consider the case where \mathbf{x} is outside the sphere (i.e., $\|\mathbf{x}\| > r$) and pick the smaller root:

$$D(t) = \langle \mathbf{x} - t\mathbf{v}, \boldsymbol{\omega} \rangle - \sqrt{\langle \mathbf{x} - t\mathbf{v}, \boldsymbol{\omega} \rangle^2 - \|\mathbf{x} - t\mathbf{v}\|^2 + r^2}, \quad (84)$$

which can be differentiated symbolically to obtain \dot{D} . For instance, when $\|\dot{\mathbf{x}}\| > 0$ and $\|\dot{\boldsymbol{\omega}}\| = 0$, it holds that

$$\dot{D} = \langle \dot{\mathbf{x}} - \mathbf{v}, \boldsymbol{\omega} \rangle - \frac{\langle \mathbf{x}, \mathbf{v} \rangle + \langle \mathbf{x}, \boldsymbol{\omega} \rangle \langle \dot{\mathbf{x}} - \mathbf{v}, \boldsymbol{\omega} \rangle - \langle \mathbf{x}, \dot{\mathbf{x}} \rangle}{\sqrt{\langle \mathbf{x}, \boldsymbol{\omega} \rangle^2 - \|\mathbf{x}\|^2 + r^2}}. \quad (85)$$

We omit the general form of \dot{D} here for notational simplicity.

Sphere (uniform scaling). When a sphere scales uniformly around its center, the ray $(\mathbf{x}, -\boldsymbol{\omega})$ intersects the sphere at time t if

$$\|\mathbf{x} - D\boldsymbol{\omega}\|^2 - (r + t)^2 = D^2 - 2\langle \mathbf{x}, \boldsymbol{\omega} \rangle D + \|\mathbf{x}\|^2 - (r + t)^2 = 0. \quad (86)$$

Considering again the case where \mathbf{x} lies outside the sphere leads to

$$D(t) = \langle \mathbf{x}, \boldsymbol{\omega} \rangle - \sqrt{t^2 + 2rt + \langle \mathbf{x}, \boldsymbol{\omega} \rangle^2 - \|\mathbf{x}\|^2 + r^2}. \quad (87)$$

Then,

$$\dot{D} = \langle \dot{\mathbf{x}}, \boldsymbol{\omega} \rangle + \langle \mathbf{x}, \dot{\boldsymbol{\omega}} \rangle - \frac{r + \langle \mathbf{x}, \boldsymbol{\omega} \rangle (\langle \dot{\mathbf{x}}, \boldsymbol{\omega} \rangle + \langle \mathbf{x}, \dot{\boldsymbol{\omega}} \rangle) - \langle \mathbf{x}, \dot{\mathbf{x}} \rangle}{\sqrt{\langle \mathbf{x}, \boldsymbol{\omega} \rangle^2 - \|\mathbf{x}\|^2 + r^2}}. \quad (88)$$